bioRxiv preprint doi: https://doi.org/10.1101/2023.10.31.564956; this version posted November 1, 2023. The copyright holder for this preprint (which was not certified by peer review) is the author/funder, who has granted bioRxiv a license to display the preprint in perpetuity. It is made available under aCC-BY-NC-ND 4.0 International license.

The N6-methyladenosine demethylase ALKBH5 regulates the hypoxic HBV transcriptome.

Senko Tsukuda[1]*, James M Harris[1], Andrea Magri[1], Peter Balfe[1], Peter AC Wing[2], Aleem Siddiqui[3], and Jane A McKeating[1,2]*.

[1]Nuffield Department of Medicine, University of Oxford, UK.
[2]Chinese Academy of Medical Sciences Oxford Institute, University of Oxford, UK.
[3] Division of Infectious Diseases and Global Public Health, University of California, CA, USA.

*Joint corresponding authors
Email: jane.mckeating@ndm.ox.ac.uk and ORCID ID: 0000-0002-7229-5886.
senko.tsukuda@ndm.ox.ac.uk and ORCID ID: 0000-0002-7289-3018

Key words: HBV, m^{6}A, ALKBH5, hypoxia, HIF

bioRxiv preprint doi: https://doi.org/10.1101/2023.10.31.564956; this version posted November 1, 2023. The copyright holder for this preprint (which was not certified by peer review) is the author/funder, who has granted bioRxiv a license to display the preprint in perpetuity. It is made available under aCC-BY-NC-ND 4.0 International license.

Abstract

Chronic hepatitis B is a global health problem and current treatments only suppress hepatitis B virus (HBV) infection, highlighting the need for new curative treatments. Oxygen levels influence HBV replication and we previously reported that hypoxia inducible factors (HIFs) activate the basal core promoter to transcribe pre-genomic RNA. Application of a probe-enriched long-read sequencing method to map the HBV transcriptome showed an increased abundance of all viral RNAs under low oxygen or hypoxic conditions. Importantly, the hypoxic-associated increase in HBV transcripts was dependent on N6-methyladenosine (m^6A) modifications and an m^6A DRACH motif in the 5' stem loop of pre-genomic RNA defined transcript half-life under hypoxic conditions. Given the essential role of m^6A modifications in the viral transcriptome we assessed the oxygen-dependent expression of RNA demethylases and bio-informatic analysis of published single cell RNA-seq of murine liver showed an increased expression of the RNA demethylase ALKBH5 in the peri-central low oxygen region. *In vitro* studies with a human hepatocyte derived HepG2 cell line showed increased ALKBH5 gene expression under hypoxic conditions. Silencing the demethylase reduced the levels of HBV pre-genomic RNA and host gene (CA9, NDRG1, VEGFA, BNIP3, FUT11, GAP and P4HA1) transcripts and this was mediated via reduced HIFα expression. In summary, our study highlights a previously unrecognized role for ALKBH5 in orchestrating viral and cellular transcriptional responses to low oxygen.

Author Summary

Oxygen levels influence HBV replication and hypoxia inducible factors (HIFs) activate HBV transcription. Long-read sequencing and mapping the HBV transcriptome showed an increased abundance of all viral RNAs under hypoxic conditions that was dependent on N6-methyladenosine modifications. Investigating the oxygen-dependent expression of RNA demethylases identified ALKBH5 as a hypoxic activated gene and silencing its expression showed a key role in regulating HBV and host gene expression under hypoxic conditions.

Abbreviations

HBV, hepatitis B virus; HCC, hepatocellular carcinoma; rcDNA, relaxed circular DNA; cccDNA, covalently closed circular DNA; pgRNA, pregenomic RNA; HBe, hepatitis B e antigen; HBx, HBV X protein; m^6A, N6-methyladenine; HIF, hypoxia-inducible factor; NTCP, sodium taurocholate cotransporting polypeptide; 2OG, 2-oxoglutarate; MeRIP, methylated RNA immunoprecipitation; CREBBP, CREB binding protein; CA9, carbonic anhydrase 9; NDRG1, N-myc downstream-regulated gene 1; PHD, prolyl hydroxylase domain proteins; VHL, von Hippel-Lindau disease tumor suppressor; METTL3/14,

bioRxiv preprint doi: https://doi.org/10.1101/2023.10.31.564956; this version posted November 1, 2023. The copyright holder for this preprint (which was not certified by peer review) is the author/funder, who has granted bioRxiv a license to display the preprint in perpetuity. It is made available under aCC-BY-NC-ND 4.0 International license.

methyltransferase-like protein 3/14; ALKBH5, α-ketoglutarate-dependent dioxygenase alk B homolog 5; FTO, fat mass and obesity-associated protein; YTHDF1-3, YTH domain containing family 1-3; YTFDC1-2, YTF domain containing1-2; WB, western blotting, siRNA, small interfering RNA; PCR, polymerase chain reaction; qPCR, quantitative PCR.

Introduction

Chronic hepatitis B (CHB) is one of the world's most economically important diseases, with 2 billion people exposed to the virus during their lifetime resulting in a global burden of >290 million chronic infections. Hepatitis B virus (HBV) replicates in the liver and chronic infection can result in progressive liver disease, cirrhosis and hepatocellular carcinoma (HCC) [1]. HBV is the prototypic member of the *hepadnaviridae* family of small enveloped hepatotropic viruses with a partial double-stranded relaxed circular DNA (rcDNA) genome. Current treatments include nucleos(t)ide analogs and interferons that suppress virus replication but are not curative largely due to the persistence of episomal HBV genomes and dysfunctional viral-specific immune responses [2].

HBV infects hepatocytes and the rcDNA genome translocates to the nucleus and is converted to covalently closed circular DNA (cccDNA) by host-DNA repair enzymes [3]. Several members of the host DNA repair pathway convert rcDNA to cccDNA that serves as the transcriptional template for all viral RNAs [4]. HBV transcribes six major RNAs of decreasing length, with a common 3' polyadenylation signal that include: pre-core (pC) that encodes e antigen; pre-genomic (pgRNA) that is translated to yield core protein and polymerase; preS1, preS2 and S RNAs encoding the surface envelope glycoproteins and X transcript for the multi-functional x protein (HBx) [5]. pgRNA contains stem loop structures at both the 5' and 3' termini that bind host factors that regulate transcript stability, including zinc finger CCHC-type Containing 14 protein that recruits terminal nucleotidyltransferase 4 [6] and the zinc finger antiviral protein that regulates RNA decay [7] (reviewed in [5]). pgRNA is encapsidated and reverse-transcribed by the viral polymerase to generate rcDNA genomes that can be enveloped and secreted as infectious particles [8].

*N*6-methyladenosine (m^6A) is the most abundant modification found on eukaryotic transcripts where it can regulate mRNA structure, stability, translation and nuclear export. m^6A modifications are regulated by the balanced activities of m^6A "writer" and "eraser" proteins. Adenosine is methylated by writers including two methyltransferase-like 3 (METTL3) and METTL14 [9] along with their cofactor Wilms tumor 1-associated protein (WTAP) [10]. This complex methylates adenosine

bioRxiv preprint doi: https://doi.org/10.1101/2023.10.31.564956; this version posted November 1, 2023. The copyright holder for this preprint (which was not certified by peer review) is the author/funder, who has granted bioRxiv a license to display the preprint in perpetuity. It is made available under aCC-BY-NC-ND 4.0 International license.

residues within the consensus DRACH (D=A, G or U; R=G or A; H=A, C or U) motif which is often located near stop codons, 3' untranslated regions and internal exons in mRNAs [11, 12]. m^{6}A modifications can be removed by erasers including the demethylases, AlkB Homolog 5 (ALKBH5) and fat mass and obesity-associated protein (FTO) [13, 14]. HBV cccDNA encodes a DRACH motif present in all viral transcripts near the common 3' polyadenylation signal in a region termed the epsilon stem loop, but notably is also found in the 5' terminal repeat at the start of the pC and pgRNA transcripts [15]. m^{6}A modified HBV RNAs are recognized by YTH domain containing protein 2 (YTHDF2) and the interferon-induced RNase, ISG20, that can process them for degradation [16]. More recently, m^{6}A modified HBV RNAs were reported to be preferentially transported from the nucleus and encapsidated [17, 18]. Collectively, these studies demonstrate an important role for these post-transcriptional modifications in multiple stages of the HBV life cycle.

Oxygen concentration varies across different tissues, with the liver receiving oxygenated blood from the hepatic artery and partially oxygen-depleted blood via the hepatic portal vein, resulting in an oxygen gradient of 8-3% across the periportal and pericentral areas, respectively [19]. This oxygen gradient associates with liver zonation, a phenomenon where hepatocytes show distinct functional and structural organization across the liver [20]. Mammalian cells adapt to low oxygen through an orchestrated transcriptional response regulated by hypoxia inducible factors (HIFs): a heterodimeric transcription factor comprising alpha (HIF-1α, HIF-2α, or HIF-3α) and beta (HIF-1β) subunits [21]. Oxygen dependent prolyl-hydroxylase (PHD) enzymes hydroxylate HIF-α subunits for proteasomal degradation and hypoxic inactivation of the PHDs stabilizes HIF-α expression leading to transcription of genes involved in metabolic processes [22]. We recently showed that HIFs bind and activate HBV cccDNA transcription both in laboratory models maintained under low oxygen and in HBV transgenic mice [23]. HIFs also suppress cccDNA deamination by Apolipoprotein B mRNA Editing Catalytic Polypeptide-like 3B (APOBEC3B) [24]. To date, studies investigating the role of m^{6}A modifications in the HBV life cycle have been performed under standard laboratory conditions of 18% oxygen, where HIFs are inactive. As the RNA demethylase ALKBH5 was previously reported to be regulated by HIF-1α [25], we studied the role of m^{6}A modifications in the HBV life cycle under low oxygen conditions that mimic the liver. Our studies identify an essential role for m^{6}A modifications in regulating the HBV transcriptome and long-read sequencing revealed oxygen- and m^{6}A-dependent regulation of canonical and non-canonical viral RNAs. We also identify a role for ALKBH5 in the regulation of HIF-1α under hypoxic conditions that impacts the abundance of HBV and cellular transcripts.

bioRxiv preprint doi: https://doi.org/10.1101/2023.10.31.564956; this version posted November 1, 2023. The copyright holder for this preprint (which was not certified by peer review) is the author/funder, who has granted bioRxiv a license to display the preprint in perpetuity. It is made available under aCC-BY-NC-ND 4.0 International license.

Results

Hypoxic regulation of the HBV transcriptome is dependent on m^{6}A modifications.

To assess the role of m^{6}A RNA modifications in HBV replication under low oxygen conditions we mutated the DRACH motifs to generate m6A-null virus as previously reported [15]. Transfecting HepG2-NTCP cells with plasmids encoding wild-type (WT) or the mutated viral genome (HBV m^{6}A-null) allowed us to generate virus for infection studies. We selected 1% oxygen as this is known to stabilise HIFα subunits and activate HIF target gene transcription [23]. HBV WT or m^{6}A-null infected cells were cultured at 18% or 1% oxygen for 72h and pgRNA quantified by PCR. To measure HIF-dependent regulation of pgRNAs the infected cells were treated with a prolyl-hydroxylase inhibitor (FG-4592) that activates HIF-signalling. Low oxygen or FG-4592 treatment induced a significant increase in the abundance of pgRNA in the WT infected cells, however, transcript levels were unchanged in the HBV m^{6}A-null infected cells (**Fig.1A**). We noted comparable expression of the HIF-target gene carbonic anhydrase 9 (*CA9*) in WT and HBV m^{6}A-null infected cells, suggesting an essential role for m^{6}A modifications in the HIF induction of pgRNA.

To explore the interplay between hypoxia and methylation status on the HBV transcriptome we used a probe-enrichment long-read sequencing approach [26] to map viral transcripts. We extended our earlier analytical pipeline to include all reported viral transcription start sites (TSS) [27, 28] and to map full-length transcripts. The sequenced libraries contained 47,697 - 119,071 reads and we noted a similar frequency of HBV reads among the samples, ranging from 41-55% of total reads (**Supplementary Table 1A)**. To compare the profile of HBV RNAs in the different samples we expressed the viral reads as transcripts per million (TPM) (**Supplementary Table 1B**). PreS2 RNAs were the most abundant transcript irrespective of hypoxic conditions or methylation status, with lower levels of pC, pgRNA, HBx and spliced RNAs in the HBV m^{6}A-null samples compared to WT although these differences were not statistically significant (**Fig.1B-C** and **Supplementary Table 1B**). A minority of viral transcripts did not map to known TSS and were classified as unmapped, with many of these encoding an S gene open reading frame (ORF) (**Supplementary Table 1B**). Mapping the spliced transcripts identified SP1 and SP14 as the most abundant (~15-30,000 TPM, respectively) with SP6, SP7, SP9 and pSP12 transcripts also detected (>1,000 TPM) (**Fig.1B-C, Supplementary Table 1B**). SP1 transcript levels were reduced in the HBV m^{6}A-null samples compared to WT, with a concomitant increase in SP14 (**Fig.1C, Supplementary Table 1B**). Differential expression analysis identified three viral transcripts, pgRNA, preS2 and

bioRxiv preprint doi: https://doi.org/10.1101/2023.10.31.564956; this version posted November 1, 2023. The copyright holder for this preprint (which was not certified by peer review) is the author/funder, who has granted bioRxiv a license to display the preprint in perpetuity. It is made available under aCC-BY-NC-ND 4.0 International license.

preS, together with the major spliced transcript SP1, that were significantly increased in HBV WT samples under hypoxia (adjusted p-values < 10^{-6}) (**Fig.1D**). In contrast, pC, preS1 or HBx transcript levels did not increase under hypoxic conditions (**Fig.1D**). HBV m^{6}A-null derived RNAs were insensitive to the low oxygen (**Fig.1D**), demonstrating a key role for m^{6}A post-transcriptional modifications in defining the hypoxic HBV transcriptome.

As methylation and hypoxia can both influence RNA stability [29, 30] we measured the half-life of HBV WT or m^{6}A-null derived transcripts under low-oxygen conditions by treating cultures with actinomycin D (**Fig.1E**). Given the overlapping nature of the HBV transcripts we can only accurately quantify pgRNA by qPCR. HBV m^{6}A-null encoded pgRNAs had a significantly shorter half-life than WT transcripts in cells cultured under standard laboratory conditions (18% O_2) (8.33 ± 0.71h v 13.9 ± 2.18h, p=0.014), consistent with reports that m^{6}A modifications reduce the stability of viral RNA [15]. Hypoxia did not alter the half-life of HBV WT pgRNA but we noted a significant reduction in m^{6}A-null pgRNA under these conditions (6.93 ± 0.64h v 8.33 ± 0.71h, p=0.044) (**Fig.1E**). In summary, these data highlight a role for oxygen-dependent processes in regulating the stability of non-methylated and methylated HBV pgRNA.

The 5' stem-loop DRACH motif regulates pgRNA abundance under hypoxic conditions.

To investigate which m^{6}A motif regulates pgRNA levels under low oxygen conditions, we transfected HepG2-NTCP cells with HBV 1.3x overlength plasmids with mutations in the DRACH motif in the 5' loop (HBV m^{6}A-5'null), the 3' loop (HBV m^{6}A-3'null) or both loops (HBV m^{6}A-null) (**Fig.2A**). Transfected HepG2-NTCP cells were cultured at 18% or 1% oxygen conditions and pgRNA along with secreted HBV DNA measured (**Fig.2B**). Measuring intracellular HBV DNA at 4h post transfection demonstrated similar efficiencies of transfection (**Supplementary Fig.1A**) and we confirmed that all samples responded to the hypoxic conditions by measuring *CA9* gene expression (**Supplementary Fig.1B**). Lower levels of pgRNA were noted in the m^{6}A-null and m^{6}A-5'null transfected cells compared to WT or m^{6}A-3'null, consistent with our earlier report showing their reduced replicative fitness (**Supplementary Fig.1B**) [15]. We observed hypoxic induction of pgRNA and extracellular HBV DNA in the WT or m^{6}A-3'null transfected cells, whilst neither m^{6}A-null nor m^{6}A-5'null showed any oxygen-dependent modulation.

We were interested to understand whether the hypoxia-associated increase in extracellular HBV DNA reflected an increase in pgRNA encapsidation. HepG2 cells

bioRxiv preprint doi: https://doi.org/10.1101/2023.10.31.564956; this version posted November 1, 2023. The copyright holder for this preprint (which was not certified by peer review) is the author/funder, who has granted bioRxiv a license to display the preprint in perpetuity. It is made available under aCC-BY-NC-ND 4.0 International license.

transfected with HBV were cultured under hypoxic conditions and the relative abundance of pgRNA in the nucleus, cytosol or within capsids measured. The majority of pgRNA was in the cytosol and this did not change under low oxygen conditions (**Fig.2C**), suggesting that hypoxia does not influence the encapsidation machinery and/or assembly processes. In summary, these data show that 5' m^{6}A modification plays an essential role in hypoxia-dependent increase in the abundance of pgRNA.

Hypoxic activation of ALKBH5 expression impacts m6A modified HBV and host transcripts.

The m^{6}A demethylase ALKBH5 is a direct target of HIF-1α [25] and is hypoxic regulated in a variety of cell lines, including breast cancer and adipocyte cells [31, 32]. We investigated ALKBH5 expression in the liver using published single cell RNA-seq data of murine liver [33]. We observed an enrichment of *Alkbh5* transcripts in the low oxygen pericentral area (PC) compared to the perivenous region (PV) (**Fig.3A**). Zonal expression of the HIF target gene, N-myc downstream regulated 1 (*Ndrg1*) was noted, whereas expression of m^{6}A demethylase Fat mass and obesity associated (*Fto*) gene was comparable across the liver lobule (**Fig.3A, Supplementary Fig.2**). To ascertain whether these observations translate to our *in vitro* model we cultured HepG2 cells at 18% and 1% oxygen and showed a significant increase in ALKBH5 gene expression in hypoxic cells (**Fig.3B**). To assess the functional consequences, we measured total m^{6}A-RNA levels by immuno-northern blotting with an anti-m6A antibody and showed a reduction in m^{6}A-modified cellular RNAs under hypoxic conditions, consistent with the increase in demethylase expression (**Fig.3C**).

To investigate whether hypoxia alters HBV pgRNA methylation status we used an m^{6}A–RNA immunoprecipitation (RIP) assay combined with qPCR and showed a significant reduction in precipitated pgRNA under hypoxic conditions (**Fig.3D**). As a control we PCR quantified the m6A modified CREBBP transcript and noted a reduction under hypoxic conditions. To investigate the potential role of ALKBH5 in regulating the abundance of HBV pgRNAs we silenced the demethylase with two independent siRNAs targeting different exons. We confirmed siRNA efficacy in cells cultured at 18% or 1% oxygen and siRNA #2 showed a greater reduction in ALKBH5 expression (**Supplementary Fig.3**). Silencing ALKBH5 blunted the hypoxic-associated increase in HBV pgRNA (**Fig.3E**), suggesting a role for this demethylase in regulating HBV RNAs under low oxygen conditions.

ALKBH5 regulates HIF-α expression.

bioRxiv preprint doi: https://doi.org/10.1101/2023.10.31.564956; this version posted November 1, 2023. The copyright holder for this preprint (which was not certified by peer review) is the author/funder, who has granted bioRxiv a license to display the preprint in perpetuity. It is made available under aCC-BY-NC-ND 4.0 International license.

As we previously identified a role for HIFs to bind and activate HBV transcription, we investigated the interplay between ALKBH5 and HIFs. *HIF-1α* mRNA is methylated in HepG2 cells and there was a trend albeit non-significant, for reduced amounts of anti-m^{6}A precipitated transcripts under hypoxic conditions (**Supplementary Fig.4A**). HepG2 cells were transfected with siRNAs targeting ALKBH5 or an irrelevant negative control (NC) and cultured at 1% oxygen for 24h to stabilize HIF expression and activate NDRG1 expression (**Fig.4A**). Cells transfected with siALKBH5 showed a significant reduction in the expression of both HIF-α isoforms and associated NDRG1 expression, whereas *HIF-1α* transcripts were unchanged (**Fig.4A**). Of note, ALKBH5 silencing did not affect the abundance or half-life of *HIF-1α* transcripts (8.9-10.1 h) (**Fig.4B**). Silencing ALKBH5 in HepG2 cells blunted the hypoxic induction of a panel of HIF target genes (*CA9*, *NDRG1*, *VEGFA*, *BNIP3*, *FUT11*, *GP1*, and *P4HA1*), demonstrating the broad impact of this demethylase to regulate HIF-transcriptional activity (**Fig.4C**).

HIF-α is hydroxylated by PHDs leading to ubiquitination and targeting for proteasomal degradation. ALKBH5 silencing had no major effects on the levels of hydroxylated HIF-1α (**Supplementary Fig.5**). To assess the role for ALKBH5 in post-transcriptional regulation of HIF-α, HepG2 cells were transfected with siALKBH5 #2 as it showed the most robust silencing. The cells were cultured under hypoxic conditions for 24h before treatment with cycloheximide (CHX) to inhibit protein synthesis. CHX treatment inhibited HIF-1α and HIF-2α expression, and their degradation was accelerated in the absence of ALKBH5 (**Fig.4D**), consistent with a role for the demethylase in destabilizing both isoforms. This conclusion is further supported by treating the cells with a proteosomal inhibitor (MG132), that induced the expression of both HIF-α isoforms, and ALKBH5 silencing delaying their expression kinetics (**Fig.4D**). Collectively, these data illustrate a key role for the ALKBH5 demethylase in regulating HIF expression and function.

Discussion

Our study shows an essential role for m^{6}A RNA modifications in regulating the hypoxic HBV transcriptome. Long-read sequencing of the HBV WT infected cells allowed us to accurately map hypoxic regulated transcripts and we observed a significant increase in pgRNA, preS2, preS and SP1 transcripts, with no change in pC, preS1, HBx or other spliced mRNAs. The oxygen-dependent enrichment of viral transcripts is not dependent on their abundance and may reflect the methylation status of the different transcripts. At the present time it is not possible to profile the m^{6}A methylation of viral RNAs using available long-read sequencing platforms. Given the overlapping nature of the HBV transcripts we can only reliably qPCR measure pgRNA and meRIP

bioRxiv preprint doi: https://doi.org/10.1101/2023.10.31.564956; this version posted November 1, 2023. The copyright holder for this preprint (which was not certified by peer review) is the author/funder, who has granted bioRxiv a license to display the preprint in perpetuity. It is made available under aCC-BY-NC-ND 4.0 International license.

assays confirm that pgRNA is m^{6}A modified. The observation that the hypoxia-mediated increase in HBV pgRNA is dependent on 5'-m^{6}A modification suggests m^{6}A specific recognition mechanisms. Wang *et al* analyzed the location of m^{6}A modifications on RNAs isolated from hypoxic HeLa cells and reported that cells undergo a reprogramming of their m^{6}A epitranscriptome by altering both the m^{6}A level at specific sites and their distribution patterns in response to hypoxia [30]. We cannot exclude that hypoxia may alter m^{6}A modified sites on HBV RNAs. Mutation of the 5'-m^{6}A DRACH HBV motif at position 1907 (A to C) is unlikely to impair HIF-1α binding to hypoxic responsive elements that are located in the basal core promoter located at residues 1751-1769. RNA decay assays showed that the stability and expression of m^{6}A-null pgRNA was reduced under low oxygen conditions and further experiments to image the intracellular location of methylated and non-methylated transcripts in infected cells may provide mechanistic insights.

Recent studies have highlighted an interplay between hypoxia signaling and m^{6}A-post transcriptional regulatory pathways; where decreased levels of m^{6}A-RNAs were seen in breast cancer cells, cardiac microvascular endothelial and cervical cancer cells [32, 34]. In contrast, increased levels of m^{6}A modified RNAs were found in human umbilical vein endothelial cells, cardiomyocytes and murine hearts under hypoxic conditions that associated with increased methyltransferase METTL3 expression [35-37]. Collectively, these studies show that hypoxic modulation of m^{6}A-RNA is dependent on both the tissue and cell type. Consistent with our observations, Wang *et al* reported a hypoxic reduction in m^{6}A modified RNAs in human hepatoma Huh-7, HepG2 and Hep3B cell lines that was partially reversed by silencing ALKBH5 [30]. Reports that m^{6}A modified RNAs are perturbed in inflammatory diseases highlight a potential therapeutic role for targeting this pathway (reviewed in [38]).

Analyzing a published single-cell RNA sequencing (scRNA-seq) data set from mouse liver [33] showed a zonation of *Alkbh5* but not *Fto*, with transcripts more abundant in the pericentral region of the liver, consistent with hypoxic regulation. ALKBH5 is a HIF target gene and its expression is induced under low oxygen conditions. ALKBH5 activity is also regulated by post-translation methylation and SUMOylation modifications that provide a further level of control over demethylase activity [39]. Our results showing reduced pgRNA levels in HBV infected ALKBH5 silenced cells under hypoxic conditions supports a positive role for this demethylase in susceptibility to viral infection. This conclusion is consistent with our earlier work that reported an increased expression of HBV antigen expressing cells in the pericentral 'high ALKBH5' areas of the liver in HBV transgenic mice [23, 24]. Liu *et al* reported that *Alkbh5* deficient mice were resistant to infection by a range of DNA and RNA viruses (VSV,

bioRxiv preprint doi: https://doi.org/10.1101/2023.10.31.564956; this version posted November 1, 2023. The copyright holder for this preprint (which was not certified by peer review) is the author/funder, who has granted bioRxiv a license to display the preprint in perpetuity. It is made available under aCC-BY-NC-ND 4.0 International license.

334 HSV-1 EMCV) that was mediated by an m^{6}A RNA-dependent down regulation of a-
335 ketoglutarate dehydrogenase (OGDH)-itaconate pathway that supports virus
336 replication [40]. The authors show that Vesicular Stomatitis Virus infection targeted
337 the ALKBH5 pathway to evade this host restriction pathway. We have limited
338 evidence for HBV infection to alter ALKBH5 expression or activity in our experiments.
339 Qu *et al* reported that HBx increased H3K4me3 modifications in the ALKBH5 promoter
340 region that associated with increased demethylase expression [41]. The authors
341 noted increased ALKBH5 expression in HBV-HCC samples, however, there were no
342 mechanistic studies to link this directly to HBx and given the hypoxic nature of HCC
343 (reviewed in [42]) this could align with a HIF-driven activation of ALKBH5 gene
344 expression.
345
346 Adenosine methylation can regulate many aspects of mRNA metabolism including
347 splicing, nuclear export, stability, and translation. Most translation events in the cell
348 occur through recognition of the cap by the eIF4F protein complex. However, it has
349 long been known that cellular states such as apoptosis, mitosis or the stress response
350 can suppress cap-dependent translation allowing selected mRNAs to be translated.
351 Recent studies reported that stress conditions, such as heat shock or amino acid
352 starvation, promote nuclear trafficking of the m^{6}A reader proteins YTHDF1 and
353 YTHDF2 [43, 44] and increase cap-independent translation of mRNAs from m^{6}A-
354 modified 5'UTR [43, 45-47]. We found that ALKBH5 silencing reduced HIF-α
355 expression without affecting RNA levels or half-life. Silencing of ALKBH5 did not alter
356 the levels of hydroxylated HIF-1α, suggesting that this demethylase does not regulate
357 PHD activity, further enzymic studies would be required to address this mechanism.
358 There is a report showing that PBMR1, a component of the chromatin remodeler
359 SWI/SNF, positively regulates HIF-1α translation through protein interaction between
360 YTHDF2 under normoxic and hypoxic conditions and HIF expression was reduced
361 when these proteins were silenced [43]. These reports are consistent with an
362 essential role for m^{6}A modified RNAs in cellular adaption to hypoxic stress. Taken
363 together, our results support a role for ALKBH5 to regulate HIF-1α stability and
364 transcriptional activity and in cellular adaption to hypoxic stress. Our findings on the
365 cross-talk of ALKBH5 and HIF signalling provide mechanistic insights into cellular
366 responses that regulate HBV replication and may be more widely applicable to other
367 liver tropic pathogens (**Fig.5**).
368

bioRxiv preprint doi: https://doi.org/10.1101/2023.10.31.564956; this version posted November 1, 2023. The copyright holder for this preprint (which was not certified by peer review) is the author/funder, who has granted bioRxiv a license to display the preprint in perpetuity. It is made available under aCC-BY-NC-ND 4.0 International license.

Materials and methods

Reagents. FG-4592 was obtained from either Selleckchem or MedChemExpress. Cyclohexamide was purchased from Abcam. siRNAs were obtained from Thermo Fisher Scientific, MG132 and actinomycin D were purchased from Sigma-Aldrich. Primary antibodies used in this study are ALKBH5 (Atlas Antibodies), β Actin (Sigma), HIF-1α (BD Bioscience), HIF-2α (NOVUS), HIF-1β (NOVUS), NDRG1 (CST), anti-m^{6}A polyclonal antibody (Synaptic Systems). HRP-conjugated secondary antibodies were purchased from DAKO.

Cell lines. HepG2-NTCP cells were maintained in Dulbecco's Modified Eagles Medium (DMEM) (ThermoFisher), containing Glutamax supplemented with 10% Fetal Bovine Serum, 50 U/ml Penicillin/Streptomycin, and non-essential amino acids. Cells were maintained in 5% CO_2 and 18% oxygen. Hypoxic treatment of cells was carried out in a hypoxic incubator (New Brunswick Galaxy 48R, Eppendorf) or a hypoxia chamber (Invivo 400, Baker-Ruskinn Technologies) at 5% CO_2 and 1% oxygen.

HBV preparation and infection. HBV was prepared from the supernatant HepG2 cells transfected HBV1.3 plasmids [15] by polyethylene glycol 8000 precipitation. Briefly, culture media was mixed with 10% PEG8000/ 2.3% NaCl and incubated at 4°C for 16h, then centrifuged at 4500 rpm for 1h at 4°C. After discarding the supernatant, the pellet was resuspended in DMEM (~200-fold concentration). The inoculum was treated with DNase at 37°C for 1h, DNA extracted and quantified by qPCR to measure HBV genome copies. HepG2-NTCP cells were seeded on collagen coated plasticware and infected with HBV (MOI of 300 or 1,000 based on genome copies) in the presence of 4% PEG8000 for 16h. Viral inoculum was removed and cells washed three times with PBS. Infected cells were maintained in 5% CO_2 and 18% oxygen and treatments applied.

Transfection. Plasmids were transfected into HepG2-NTCP cells using either polyethylenimine (PEI) or FuGENE HD Transfection Reagent (Promega) according to the manufacturer's protocol. siRNAs for ALKBH5 (1; s29686 and #2; s29688) and non-targeting control (4390844) were obtained from Thermo Fisher Scientific and transfected using DharmaFECT 4 Transfection Reagent (Horizon Discovery) according to the manufacturer's protocol.

Quantitative PCR. Total cellular RNA was extracted using an RNeasy kit (Qiagen), then treated with TURBO DNA-free (Thermo Fisher Scientific), and the RNA reverse transcribed using a cDNA synthesis kit (PCR Biosystems) according to the

bioRxiv preprint doi: https://doi.org/10.1101/2023.10.31.564956; this version posted November 1, 2023. The copyright holder for this preprint (which was not certified by peer review) is the author/funder, who has granted bioRxiv a license to display the preprint in perpetuity. It is made available under aCC-BY-NC-ND 4.0 International license.

manufacturer's protocol. Cellular DNA was extracted using QIAamp DNA kit (Qiagen). Gene expression was quantified using a SyGreen Blue Mix (PCR Biosystems) with the oligonucleotides listed below and a qPCR program of 95°C for 2 min followed by 45 cycles at 95°C for 5 sec, 60°C for 30 sec. Changes in gene expression were calculated by the ΔΔCt method relative to a housekeeper gene, β2-microglobulin (B2M).

PacBio long read sequencing and analysis. HBV specific oligonucleotide enrichment and subsequent long-read sequencing and analysis was performed as reported [48]. Briefly, RNAs were prepared from normoxic or hypoxic HepG2-NTCP cells transfected with HBV HBV1.3 WT or m6-null constructs and 150ng of RNA reverse transcribed with barcoded sequencing primers. Oligonucleotide enrichment of HBV RNAs was performed as previously described [49]. Samples were sequenced using a Sequel II instrument to generate a PacBio 'Hifi library'. Reads were mapped to the HBV reference genome (genotype D3, ayw strain) using minimap2 [50, 51]. HBV reads were assigned to previously reported transcription start sites to identify canonical transcripts [27] and splice junctions enumerated to identify non-canonical RNAs [51], incomplete sequences that did not encode the expected length of transcript were discounted. Differential gene expression was performed using the Voom function in Limma (Bioconductor EdgeR script). The sequencing data is available via the SRA at NCBI (BioProject ID: PRJNA1000182).

Fractionation of HBV pgRNA in the nucleus, cytosol and core particles. HepG2-NTCP cells transfected with HBV1.3 plasmid were washed with PBS and lysed in 50 mM Tris-HCl, pH 8.0, and 1% NP-40 with protease inhibitor cocktail. After incubating cells at 4°C for 20 min in the culture plate, the lysate was centrifuged for 5 min at 14,000 rpm. The pellet was the nuclear fraction and RNA extracted using Trizol. HBV core particles were isolated from the supernatant according to the protocol described by Belloni et al [52]. Briefly, 100 mM CaCl2, DNase I, and RNase A were added to the supernatant and incubated for at 37°C for 2 h. The supernatant was the incubated in 5 mM EDTA, 7% PEG8000,1.75M NaCl, at 4°C for 2 h. After centrifugation at 13,000 rpm for 30 min at 4°C, the supernatant was discarded and the capsid-containing pellet resuspended in TNE buffer (10 mM Tris-HCl (pH 8) 1mM EDTA, proteinase K), and RNA was extracted using Trizol. To calculate pgRNA levels in the cytosol, total HBV RNAs were extracted from the cells using Trizol and pgRNA quantities in the nucleus and capsid subtracted after quantifying by qPCR.

Extracellular HBV DNA quantification. Extracellular HBV DNA was quantified according to the protocol described previously [53]. Briefly, culture supernatant was treated with DNase I (Thermo Fisher Scientific) at 37°C for 60 minutes, then treated

bioRxiv preprint doi: https://doi.org/10.1101/2023.10.31.564956; this version posted November 1, 2023. The copyright holder for this preprint (which was not certified by peer review) is the author/funder, who has granted bioRxiv a license to display the preprint in perpetuity. It is made available under aCC-BY-NC-ND 4.0 International license.

with 2x lysis buffer (100 mM Tris-HCL (pH7.4), 50 mM KCl, 0.25% Triton X-100, and 40% glycerol) containing 1mM EDTA. HBV DNA was amplified by qPCR using primers for HBV rcDNA and quantified against a DNA referent standard curve.

SDS-PAGE and western blot. Samples were lysed in RIPA buffer (50 mM Tris (pH 8.0), 150 mM NaCl, 1% Nonidet P-40, 0.5% sodium deoxycholate, and 0.1% sodium dodecyl sulphate) supplemented with protease inhibitor cocktail tablets (Roche). 4x Laemmli reducing buffer was added to samples before heating at 95°C for 10 min. Proteins were separated on 8 or 14% polyacrylamide gel and transferred to activated 0.45 µm PVDF membranes (Amersham, UK). Membranes were blocked in 5% skimmed milk and proteins detected using specific primary and HRP-secondary antibodies. Proteins were detected using SuperSignal West Pico chemiluminescent substrate kit (Pierce) and images collected on a G:Box mini (Syngene).

Immuno northern assay. 10 µg of RNA was electrophoresed in a 1 % MOPS agarose gel containing 2.2 M formaldehyde. 18 S and 28 S ribosomal RNA species were visualized under UV light after electrophoresis to verify the amount of RNA loaded and to assess degradation. After denaturation with 50 mM NaOH for 5 min, RNAs were transferred to a nylon membrane by capillary transfer using 20× SSC buffer. After UV crosslinking, the membrane was blocked in 5% skimmed milk and incubated with an anti-m^{6}A polyclonal antibody (Synaptic Systems) and HRP-secondary antibodies. Signals were realised using a SuperSignal West Pico chemiluminescent substrate kit (Pierce) and images collected on a G:Box mini (Syngene).

MeRIP. Total cellular RNA was extracted using an RNeasy (Qiagen) kit and a TURBO DNA-free Kit (Thermo Fisher Scientific), the RNA was then further purified using RNeasy kit. 2 µg of RNA was incubated overnight at 4°C with protein A agarose beads treated with Rabbit IgG or anti-m^{6}A polyclonal antibody (Synaptic Systems) in MeRIP buffer (Tris-HCl (pH 8.0),150 mM NaCl,0.1% NP-40, 1mM EDTA) supplemented with RNase inhibitor (Promega). Beads were washed 5 times with MeRIP buffer and bound RNA eluted by 6.7 mM m^{6}A sodium salt. Eluted RNA was purified using a Qiagen RNA extraction kit and quantified by qPCR. Quantities of HBV RNA, *CREBBP*, *HPRT1*, and *HIF-1a* were calculated relative to input total RNA.

bioRxiv preprint doi: https://doi.org/10.1101/2023.10.31.564956; this version posted November 1, 2023. The copyright holder for this preprint (which was not certified by peer review) is the author/funder, who has granted bioRxiv a license to display the preprint in perpetuity. It is made available under aCC-BY-NC-ND 4.0 International license.

Figure legends

Figure 1. Hypoxic regulation of the HBV transcriptome is dependent on m^{6}A methylation. (**A**) Schematic of HBV DRACH mutations in 5′ and 3′ pgRNA stem loops and protocol for HBV infection. HepG2-NTCP cells were infected with HBV wild type (WT) or m^{6}A-null and cultured at 18%, 1% oxygen or treated with FG-4592 (30 μM) for 72h. pgRNA and HIF-regulated gene carbonic anhydrase 9 (*CA9*) transcripts were measured by qPCR. Data are expressed relative to 18% oxygen for each condition and presented as mean ± S.D. of n=3 from three independent experiments with statistical significance determined using a two-way ANOVA. * $p < 0.05$, ** $p < 0.01$, *** $p < 0.001$, **** $p < 0.0001$. (**B**) Long-read sequence analysis of HBV transcriptome. Relative frequency of canonical (left) and non-canonical (right) HBV reads in HBV WT or m^{6}A-null expressing HepG2 cells cultured at 18% or 1% oxygen. (**C**) Bubble heat map denoting the HBV transcript abundance of HBV WT and m^{6}A-null samples cultured at 18% and 1% oxygen. The data is presented as the mean transcripts per million (TPM) from n=3 independent samples with the exception of WT at 1% oxygen where n=2. (**D**) Differential gene expression of hypoxic regulated HBV WT and m^{6}A-null RNAs, where the X axis denotes differences between samples (Log_2-Fold Change) and the Y axis the adjusted probability of the changes seen (-log_{10} (adjusted p-value). (**E**) HBV pgRNA half-life. HepG2-NTCP cells transfected with HBV WT plasmid were incubated at 18% or 1% oxygen conditions for 48h and cells harvested at 0, 6, 12, and 24h post actinomycin D (Act D) treatment. pgRNA relative to a housekeeping gene B2M was quantified by qPCR and half-life presented as the mean ± S.D. of n=9 from three independent experiments. n.s., not significant * $p < 0.05$, by unpaired Student's t test.

Figure 2. Hypoxic dependent increase in HBV pgRNA and secreted viral DNA is dependent on 5′ m^{6}A methylation. (**A**) Schematic of HBV plasmids indicating the location of the A-C mutation of the 5′ and 3′ m^{6}A sites in pgRNA. Circles represent WT (green) and the C mutation (red). HepG2-NTCP cells were transfected with HBV plasmids for 4h and incubated for an additional 20h at 18% oxygen, before transfer to 18% or 1% oxygen for 72h. (**B**) Intracellular pgRNA and secreted HBV DNA were quantified by qPCR and the data presented as mean ± S.D. of three independent experiments with statistical significance determined using Mann-Whitney tests, with Bonferroni correction for multiple comparisons. * $p<0.05$, ** $p < 0.01$, *** $p < 0.001$, **** $p < 0.0001$. (**C**) HepG2-NTCP cells were prepared as shown in A, and RNA extracted from the isolated cellular fractions (see methods), treated with TURBO DNase to remove any contaminating plasmid DNA and pgRNA quantified by qPCR. Data were obtained from n=5 independent samples and presented as mean ± S.D.

bioRxiv preprint doi: https://doi.org/10.1101/2023.10.31.564956; this version posted November 1, 2023. The copyright holder for this preprint (which was not certified by peer review) is the author/funder, who has granted bioRxiv a license to display the preprint in perpetuity. It is made available under aCC-BY-NC-ND 4.0 International license.

Figure 3. Hypoxic activation of ALKBH5 regulates methylation and abundance of HBV pgRNA. (**A**) Liver zonation of the RNA demethylases ALKBH5 and FTO based on scRNA-seq data from mouse liver [33]. (**B**) HepG2-NTCP cells were cultured at 18% or 1% oxygen conditions for 72h with ALKBH5 and FTO transcript levels (left) and ALKBH5 protein (right) measured. Data are expressed relative to a housekeeping gene *B2M* and presented as mean ± S.D. of n=4 from 2 experiments with statistical significance determined using Mann-Whitney tests, with Bonferroni correction for multiple comparisons, *** $p < 0.01$. (**C**) m^6A-modified RNAs. RNA was extracted from HepG2-NTCP cells cultured under 18% or 1% oxygen conditions for 72h, TURBO DNase treated and subjected to immuno-northern blotting using m^6A antibody (left). Densitometric quantification of northern blots was performed and data expressed relative to 18% oxygen. Data is shown as the mean ± S.D. of 4 independent experiments with statistical significance determined using Mann-Whitney test. * $p < 0.05$. (**D**) Quantification of methylated HBV pgRNA. HepG2-NTCP cells were transfected with HBV WT plasmid for 18h, cultured at 18% or 1% oxygen for 72h. RNA was extracted, TURBO DNase treated and subjected to Methylated RNA immunoprecipitation (MeRIP) assay using anti-m^6A antibody. Data presented are the mean ± S.D. of n=6 samples from independent 3 experiments with statistical significance determined using Mann-Whitney tests and Bonferroni correction for multiple comparisons. ** $p < 0.01$. (**E**) HepG2-NTCP cells were transfected with siRNAs (NC; Non-targeting, ALK; ALKBH5) for 6h, followed by delivery of HBV WT plasmid and cultured at 18% or 1% oxygen for 72h. RNA was extracted, TURBO DNase digested and pgRNA quantified by qPCR. Data are expressed relative to a house keeping gene *B2M* and presented as the mean ± S.D. of n=9 samples from 3 independent experiments with statistical significance determined using Mann-Whitney tests and Bonferroni correction for multiple comparisons. * $p < 0.05$, **** $p < 0.0001$.

Figure 4. ALKBH5 regulates HIFα expression under hypoxic conditions. (**A**) HIF-α expression in ALKBH5 silenced cells. HepG2-NTCP cells were transfected with ALKBH5 specific siRNAs for 48h and cultured under 1% oxygen for 12 or 24h. Samples were probed for HIF-1α, HIF-2α, NDRG1, ALKBH5 and β-Actin by western blotting and protein expression quantified by densitometry. HIF-1α mRNA was measured by qPCR. Data is expressed relative to 24h hypoxic siNC samples and represents the mean ± S.D. from 3 independent experiments. Statistical significance was determined using a two-way ANOVA. * $p < 0.05$, ** $p < 0.01$. (**B**) HIF-1α RNA stability in ALKBH5 silenced cells. HepG2-NTCP cells transfected with ALKBH5 siRNAs were treated with Act D as shown in Fig.1C, and HIF-1α mRNA levels quantified by qPCR and expressed relative to a housekeeping gene *B2M*. Data is shown relative to

bioRxiv preprint doi: https://doi.org/10.1101/2023.10.31.564956; this version posted November 1, 2023. The copyright holder for this preprint (which was not certified by peer review) is the author/funder, who has granted bioRxiv a license to display the preprint in perpetuity. It is made available under aCC-BY-NC-ND 4.0 International license.

0h in each condition and expressed as mean ± S.D. from 2 independent experiments. (**C**) Expression of HIF-regulated genes in ALKBH5 silenced cells. HepG2-NTCP cells were prepared as Fig.3E, and indicated gene transcripts quantified by qPCR with data expressed relative to siNC under hypoxia and represent the mean ± S.D. of samples from 3 independent experiments. (**D**) HIF-1α protein expression in ALKBH5 silenced cells. HepG2-NTCP cells were cultured in 1% oxygen for 24h and treated with cycloheximide (CHX, 20 μg/mL) or MG132 (20 μM) for the indicated times. Samples were collected and probed for HIF-1α, HIF-2α, ALKBH5 and β-Actin by western blotting. Different exposure times for the top and bottom panels were used.

Figure 5. Cartoon depicting the impact of hepatic oxygen gradient on HIF signaling, RNA demethylase gene expression and m^{6}A modified HBV RNAs.

Acknowledgements

We thank Ulla Protzer (TUM, Germany) for providing HBV stocks, Stephan Urban (University of Heidelberg) for HepG2-NTCP cells, Azim Ansari for the enrichment probes and Esther Ng for advice in analysing and mapping HBV sequences. The McKeating laboratory is funded by a Wellcome Investigator Award 200838/Z/16/Z, Chinese Academy of Medical Sciences Innovation Fund for Medical Science, China (grant number: 2018-I2M-2-002), AM is supported by the John Black Foundation. AS is supported by and NIH AI139234 grant.

Declaration of interest

The authors disclose no conflicts of interest.

References

1. Merson J. Charting a new frontier in chronic hepatitis B research to improve lives worldwide. Nature outlook 2022.

2. Levrero M, Subic M, Villeret F, Zoulim F. Perspectives and limitations for nucleo(t)side analogs in future HBV therapies. Curr Opin Virol. 2018;30:80-9. Epub 2018/05/20. doi: 10.1016/j.coviro.2018.04.006. PubMed PMID: 29777955.

3. Seeger C, Mason WS. Molecular biology of hepatitis B virus infection. Virology. 2015;479-480:672-86. Epub 20150307. doi: 10.1016/j.virol.2015.02.031. PubMed PMID: 25759099; PubMed Central PMCID: PMCPMC4424072.

4. Wei L, Ploss A. Hepatitis B virus cccDNA is formed through distinct repair processes of each strand. Nat Commun. 2021;12(1):1591. Epub 20210311. doi: 10.1038/s41467-021-21850-9. PubMed PMID: 33707452; PubMed Central PMCID: PMCPMC7952586.

bioRxiv preprint doi: https://doi.org/10.1101/2023.10.31.564956; this version posted November 1, 2023. The copyright holder for this preprint (which was not certified by peer review) is the author/funder, who has granted bioRxiv a license to display the preprint in perpetuity. It is made available under aCC-BY-NC-ND 4.0 International license.

5. Tsukuda S, Watashi K. Hepatitis B virus biology and life cycle. Antiviral Res. 2020;182:104925. Epub 2020/09/01. doi: 10.1016/j.antiviral.2020.104925. PubMed PMID: 32866519.

6. Kim D, Lee YS, Jung SJ, Yeo J, Seo JJ, Lee YY, et al. Viral hijacking of the TENT4-ZCCHC14 complex protects viral RNAs via mixed tailing. Nat Struct Mol Biol. 2020;27(6):581-8. Epub 2020/05/27. doi: 10.1038/s41594-020-0427-3. PubMed PMID: 32451488.

7. Mao R, Nie H, Cai D, Zhang J, Liu H, Yan R, et al. Inhibition of hepatitis B virus replication by the host zinc finger antiviral protein. PLoS Pathog. 2013;9(7):e1003494. Epub 2013/07/16. doi: 10.1371/journal.ppat.1003494. PubMed PMID: 23853601; PubMed Central PMCID: PMCPMC3708887.

8. Selzer L, Zlotnick A. Assembly and Release of Hepatitis B Virus. Cold Spring Harb Perspect Med. 2015;5(12). Epub 20151109. doi: 10.1101/cshperspect.a021394. PubMed PMID: 26552701; PubMed Central PMCID: PMCPMC4665036.

9. Liu X, Sun H, Qi J, Wang L, He S, Liu J, et al. Sequential introduction of reprogramming factors reveals a time-sensitive requirement for individual factors and a sequential EMT-MET mechanism for optimal reprogramming. Nat Cell Biol. 2013;15(7):829-38. Epub 2013/05/28. doi: 10.1038/ncb2765. PubMed PMID: 23708003.

10. Ping XL, Sun BF, Wang L, Xiao W, Yang X, Wang WJ, et al. Mammalian WTAP is a regulatory subunit of the RNA N6-methyladenosine methyltransferase. Cell Res. 2014;24(2):177-89. Epub 2014/01/11. doi: 10.1038/cr.2014.3. PubMed PMID: 24407421; PubMed Central PMCID: PMCPMC3915904.

11. Dominissini D, Moshitch-Moshkovitz S, Schwartz S, Salmon-Divon M, Ungar L, Osenberg S, et al. Topology of the human and mouse m6A RNA methylomes revealed by m6A-seq. Nature. 2012;485(7397):201-6. Epub 2012/05/12. doi: 10.1038/nature11112. PubMed PMID: 22575960.

12. Meyer KD, Saletore Y, Zumbo P, Elemento O, Mason CE, Jaffrey SR. Comprehensive analysis of mRNA methylation reveals enrichment in 3' UTRs and near stop codons. Cell. 2012;149(7):1635-46. Epub 2012/05/23. doi: 10.1016/j.cell.2012.05.003. PubMed PMID: 22608085; PubMed Central PMCID: PMCPMC3383396.

13. Jia G, Fu Y, Zhao X, Dai Q, Zheng G, Yang Y, et al. N6-methyladenosine in nuclear RNA is a major substrate of the obesity-associated FTO. Nat Chem Biol. 2011;7(12):885-7. Epub 2011/10/18. doi: 10.1038/nchembio.687. PubMed PMID: 22002720; PubMed Central PMCID: PMCPMC3218240.

14. Zheng G, Dahl JA, Niu Y, Fedorcsak P, Huang CM, Li CJ, et al. ALKBH5 is a mammalian RNA demethylase that impacts RNA metabolism and mouse fertility. Mol

bioRxiv preprint doi: https://doi.org/10.1101/2023.10.31.564956; this version posted November 1, 2023. The copyright holder for this preprint (which was not certified by peer review) is the author/funder, who has granted bioRxiv a license to display the preprint in perpetuity. It is made available under aCC-BY-NC-ND 4.0 International license.

Cell. 2013;49(1):18-29. Epub 2012/11/28. doi: 10.1016/j.molcel.2012.10.015. PubMed PMID: 23177736; PubMed Central PMCID: PMCPMC3646334.

15. Imam H, Khan M, Gokhale NS, McIntyre ABR, Kim GW, Jang JY, et al. N6-methyladenosine modification of hepatitis B virus RNA differentially regulates the viral life cycle. Proc Natl Acad Sci U S A. 2018;115(35):8829-34. Epub 2018/08/15. doi: 10.1073/pnas.1808319115. PubMed PMID: 30104368; PubMed Central PMCID: PMCPMC6126736.

16. Imam H, Kim GW, Mir SA, Khan M, Siddiqui A. Interferon-stimulated gene 20 (ISG20) selectively degrades N6-methyladenosine modified Hepatitis B Virus transcripts. PLoS Pathog. 2020;16(2):e1008338. Epub 2020/02/15. doi: 10.1371/journal.ppat.1008338. PubMed PMID: 32059034; PubMed Central PMCID: PMCPMC7046284.

17. Kim GW, Imam H, Siddiqui A. The RNA Binding Proteins YTHDC1 and FMRP Regulate the Nuclear Export of N(6)-Methyladenosine-Modified Hepatitis B Virus Transcripts and Affect the Viral Life Cycle. J Virol. 2021;95(13):e0009721. Epub 2021/04/23. doi: 10.1128/JVI.00097-21. PubMed PMID: 33883220; PubMed Central PMCID: PMCPMC8316146.

18. Kim GW, Moon JS, Siddiqui A. N6-methyladenosine modification of the 5' epsilon structure of the HBV pregenome RNA regulates its encapsidation by the viral core protein. Proc Natl Acad Sci U S A. 2022;119(7). Epub 2022/02/10. doi: 10.1073/pnas.2120485119. PubMed PMID: 35135882; PubMed Central PMCID: PMCPMC8851549.

19. Paris J, Henderson NC. Liver zonation, revisited. Hepatology. 2022;76(4):1219-30. Epub 20220306. doi: 10.1002/hep.32408. PubMed PMID: 35175659; PubMed Central PMCID: PMCPMC9790419.

20. Jungermann K, Kietzmann T. Zonation of parenchymal and nonparenchymal metabolism in liver. Annu Rev Nutr. 1996;16:179-203. Epub 1996/01/01. doi: 10.1146/annurev.nu.16.070196.001143. PubMed PMID: 8839925.

21. Prabhakar NR, Semenza GL. Adaptive and maladaptive cardiorespiratory responses to continuous and intermittent hypoxia mediated by hypoxia-inducible factors 1 and 2. Physiol Rev. 2012;92(3):967-1003. doi: 10.1152/physrev.00030.2011. PubMed PMID: 22811423; PubMed Central PMCID: PMCPMC3893888.

22. Palazon A, Goldrath AW, Nizet V, Johnson RS. HIF transcription factors, inflammation, and immunity. Immunity. 2014;41(4):518-28. Epub 2014/11/05. doi: 10.1016/j.immuni.2014.09.008. PubMed PMID: 25367569; PubMed Central PMCID: PMCPMC4346319.

23. Wing PAC, Liu PJ, Harris JM, Magri A, Michler T, Zhuang X, et al. Hypoxia inducible factors regulate hepatitis B virus replication by activating the basal core

bioRxiv preprint doi: https://doi.org/10.1101/2023.10.31.564956; this version posted November 1, 2023. The copyright holder for this preprint (which was not certified by peer review) is the author/funder, who has granted bioRxiv a license to display the preprint in perpetuity. It is made available under aCC-BY-NC-ND 4.0 International license.

promoter. J Hepatol. 2021;75(1):64-73. Epub 2021/02/01. doi: 10.1016/j.jhep.2020.12.034. PubMed PMID: 33516779; PubMed Central PMCID: PMCPMC8214165.

24. Riedl T, Faure-Dupuy S, Rolland M, Schuehle S, Hizir Z, Calderazzo S, et al. Hypoxia-Inducible Factor 1 Alpha-Mediated RelB/APOBEC3B Down-regulation Allows Hepatitis B Virus Persistence. Hepatology. 2021;74(4):1766-81. Epub 20210815. doi: 10.1002/hep.31902. PubMed PMID: 33991110; PubMed Central PMCID: PMCPMC7611739.

25. Thalhammer A, Bencokova Z, Poole R, Loenarz C, Adam J, O'Flaherty L, et al. Human AlkB homologue 5 is a nuclear 2-oxoglutarate dependent oxygenase and a direct target of hypoxia-inducible factor 1alpha (HIF-1alpha). PLoS One. 2011;6(1):e16210. Epub 2011/01/26. doi: 10.1371/journal.pone.0016210. PubMed PMID: 21264265; PubMed Central PMCID: PMCPMC3021549.

26. Ng E, Dobrica MO, Harris JM, Wu Y, Tsukuda S, Wing PAC, et al. An enrichment protocol and analysis pipeline for long read sequencing of the hepatitis B virus transcriptome. J Gen Virol. 2023;104(5). doi: 10.1099/jgv.0.001856. PubMed PMID: 37196057.

27. Altinel K, Hashimoto K, Wei Y, Neuveut C, Gupta I, Suzuki AM, et al. Single-Nucleotide Resolution Mapping of Hepatitis B Virus Promoters in Infected Human Livers and Hepatocellular Carcinoma. J Virol. 2016;90(23):10811-22. Epub 2016/09/30. doi: 10.1128/JVI.01625-16. PubMed PMID: 27681123; PubMed Central PMCID: PMCPMC5110153.

28. Lim CS, Sozzi V, Littlejohn M, Yuen LKW, Warner N, Betz-Stablein B, et al. Quantitative analysis of the splice variants expressed by the major hepatitis B virus genotypes. Microb Genom. 2021;7(1). doi: 10.1099/mgen.0.000492. PubMed PMID: 33439114; PubMed Central PMCID: PMCPMC8115900.

29. Fry NJ, Law BA, Ilkayeva OR, Holley CL, Mansfield KD. N(6)-methyladenosine is required for the hypoxic stabilization of specific mRNAs. RNA. 2017;23(9):1444-55. Epub 2017/06/15. doi: 10.1261/rna.061044.117. PubMed PMID: 28611253; PubMed Central PMCID: PMCPMC5558913.

30. Wang YJ, Yang B, Lai Q, Shi JF, Peng JY, Zhang Y, et al. Reprogramming of m(6)A epitranscriptome is crucial for shaping of transcriptome and proteome in response to hypoxia. RNA Biol. 2021;18(1):131-43. Epub 2020/08/05. doi: 10.1080/15476286.2020.1804697. PubMed PMID: 32746693; PubMed Central PMCID: PMCPMC7834094.

31. Chen TY, Sun D, Lin WS, Lin YL, Chao YM, Chen SY, et al. Glucosamine regulation of fibroblast growth factor 21 expression in liver and adipose tissues. Biochem Biophys Res Commun. 2020;529(3):714-9. Epub 20200718. doi: 10.1016/j.bbrc.2020.06.070. PubMed PMID: 32736697.

bioRxiv preprint doi: https://doi.org/10.1101/2023.10.31.564956; this version posted November 1, 2023. The copyright holder for this preprint (which was not certified by peer review) is the author/funder, who has granted bioRxiv a license to display the preprint in perpetuity. It is made available under aCC-BY-NC-ND 4.0 International license.

716 32. Zhang C, Samanta D, Lu H, Bullen JW, Zhang H, Chen I, et al. Hypoxia
717 induces the breast cancer stem cell phenotype by HIF-dependent and ALKBH5-
718 mediated m(6)A-demethylation of NANOG mRNA. Proc Natl Acad Sci U S A.
719 2016;113(14):E2047-56. Epub 2016/03/24. doi: 10.1073/pnas.1602883113.
720 PubMed PMID: 27001847; PubMed Central PMCID: PMCPMC4833258.
721 33. Halpern KB, Shenhav R, Matcovitch-Natan O, Toth B, Lemze D, Golan M, et
722 al. Single-cell spatial reconstruction reveals global division of labour in the
723 mammalian liver. Nature. 2017;542(7641):352-6. Epub 2017/02/07. doi:
724 10.1038/nature21065. PubMed PMID: 28166538; PubMed Central PMCID:
725 PMCPMC5321580.
726 34. Zhao Y, Hu J, Sun X, Yang K, Yang L, Kong L, et al. Loss of m6A demethylase
727 ALKBH5 promotes post-ischemic angiogenesis via post-transcriptional stabilization of
728 WNT5A. Clin Transl Med. 2021;11(5):e402. Epub 2021/05/29. doi:
729 10.1002/ctm2.402. PubMed PMID: 34047466; PubMed Central PMCID:
730 PMCPMC8087997.
731 35. Song H, Feng X, Zhang H, Luo Y, Huang J, Lin M, et al. METTL3 and ALKBH5
732 oppositely regulate m(6)A modification of TFEB mRNA, which dictates the fate of
733 hypoxia/reoxygenation-treated cardiomyocytes. Autophagy. 2019;15(8):1419-37.
734 Epub 2019/03/15. doi: 10.1080/15548627.2019.1586246. PubMed PMID:
735 30870073; PubMed Central PMCID: PMCPMC6613905.
736 36. Yao MD, Jiang Q, Ma Y, Liu C, Zhu CY, Sun YN, et al. Role of METTL3-
737 Dependent N(6)-Methyladenosine mRNA Modification in the Promotion of
738 Angiogenesis. Mol Ther. 2020;28(10):2191-202. Epub 2020/08/07. doi:
739 10.1016/j.ymthe.2020.07.022. PubMed PMID: 32755566; PubMed Central PMCID:
740 PMCPMC7545007.
741 37. Ye F, Wang X, Tu S, Zeng L, Deng X, Luo W, et al. The effects of NCBP3 on
742 METTL3-mediated m6A RNA methylation to enhance translation process in hypoxic
743 cardiomyocytes. J Cell Mol Med. 2021;25(18):8920-8. Epub 2021/08/13. doi:
744 10.1111/jcmm.16852. PubMed PMID: 34382339; PubMed Central PMCID:
745 PMCPMC8435433.
746 38. Zhang Y, Chen W, Zheng X, Guo Y, Cao J, Zhang Y, et al. Regulatory role
747 and mechanism of m(6)A RNA modification in human metabolic diseases. Mol Ther
748 Oncolytics. 2021;22:52-63. Epub 2021/09/07. doi: 10.1016/j.omto.2021.05.003.
749 PubMed PMID: 34485686; PubMed Central PMCID: PMCPMC8399361.
750 39. Yu F, Wei J, Cui X, Yu C, Ni W, Bungert J, et al. Post-translational modification
751 of RNA m6A demethylase ALKBH5 regulates ROS-induced DNA damage response.
752 Nucleic Acids Res. 2021;49(10):5779-97. doi: 10.1093/nar/gkab415. PubMed PMID:
753 34048572; PubMed Central PMCID: PMCPMC8191756.

bioRxiv preprint doi: https://doi.org/10.1101/2023.10.31.564956; this version posted November 1, 2023. The copyright holder for this preprint (which was not certified by peer review) is the author/funder, who has granted bioRxiv a license to display the preprint in perpetuity. It is made available under aCC-BY-NC-ND 4.0 International license.

754 40. Liu Y, You Y, Lu Z, Yang J, Li P, Liu L, et al. N (6)-methyladenosine RNA
755 modification-mediated cellular metabolism rewiring inhibits viral replication. Science.
756 2019;365(6458):1171-6. Epub 20190822. doi: 10.1126/science.aax4468. PubMed
757 PMID: 31439758.
758 41. Qu S, Jin L, Huang H, Lin J, Gao W, Zeng Z. A positive-feedback loop between
759 HBx and ALKBH5 promotes hepatocellular carcinogenesis. BMC Cancer.
760 2021;21(1):686. Epub 2021/06/12. doi: 10.1186/s12885-021-08449-5. PubMed
761 PMID: 34112124; PubMed Central PMCID: PMCPMC8194239.
762 42. Ringelhan M, McKeating JA, Protzer U. Viral hepatitis and liver cancer. Philos
763 Trans R Soc Lond B Biol Sci. 2017;372(1732). doi: 10.1098/rstb.2016.0274. PubMed
764 PMID: 28893941; PubMed Central PMCID: PMCPMC5597741.
765 43. Shmakova A, Frost M, Batie M, Kenneth NS, Rocha S. PBRM1 Cooperates
766 with YTHDF2 to Control HIF-1alpha Protein Translation. Cells. 2021;10(6). Epub
767 20210608. doi: 10.3390/cells10061425. PubMed PMID: 34200988; PubMed Central
768 PMCID: PMCPMC8228889.
769 44. Zhou J, Wan J, Gao X, Zhang X, Jaffrey SR, Qian SB. Dynamic m(6)A mRNA
770 methylation directs translational control of heat shock response. Nature.
771 2015;526(7574):591-4. Epub 2015/10/13. doi: 10.1038/nature15377. PubMed
772 PMID: 26458103; PubMed Central PMCID: PMCPMC4851248.
773 45. Meyer KD, Patil DP, Zhou J, Zinoviev A, Skabkin MA, Elemento O, et al. 5'
774 UTR m(6)A Promotes Cap-Independent Translation. Cell. 2015;163(4):999-1010.
775 Epub 2015/11/26. doi: 10.1016/j.cell.2015.10.012. PubMed PMID: 26593424;
776 PubMed Central PMCID: PMCPMC4695625.
777 46. Wang X, Zhao BS, Roundtree IA, Lu Z, Han D, Ma H, et al. N(6)-
778 methyladenosine Modulates Messenger RNA Translation Efficiency. Cell.
779 2015;161(6):1388-99. Epub 2015/06/06. doi: 10.1016/j.cell.2015.05.014. PubMed
780 PMID: 26046440; PubMed Central PMCID: PMCPMC4825696.
781 47. Zhou J, Wan J, Shu XE, Mao Y, Liu XM, Yuan X, et al. N(6)-Methyladenosine
782 Guides mRNA Alternative Translation during Integrated Stress Response. Mol Cell.
783 2018;69(4):636-47 e7. Epub 2018/02/13. doi: 10.1016/j.molcel.2018.01.019.
784 PubMed PMID: 29429926; PubMed Central PMCID: PMCPMC5816726.
785 48. Ng E, Dobrica M-O, Harris JM, Wu Y, Tsukuda S, Wing PAC, et al. An
786 enrichment protocol and analysis pipeline for long read sequencing of the hepatitis B
787 virus transcriptome. Journal of General Virology. 2023;104(5). doi:
788 10.1099/jgv.0.001856.
789 49. Lumley SF, Jennings D, Waddilove E, Trebes A, Delphin M, Downs LO, et al.
790 Pan-genotypic probe-based enrichment to improve efficiency of Hepatitis B virus
791 sequencing. BioRxiv. 2023. doi: 10.1101/2023.02.20.529276.

bioRxiv preprint doi: https://doi.org/10.1101/2023.10.31.564956; this version posted November 1, 2023. The copyright holder for this preprint (which was not certified by peer review) is the author/funder, who has granted bioRxiv a license to display the preprint in perpetuity. It is made available under aCC-BY-NC-ND 4.0 International license.

50. Li H. Minimap2: pairwise alignment for nucleotide sequences. Bioinformatics. 2018;34(18):3094-100. Epub 2018/05/12. doi: 10.1093/bioinformatics/bty191. PubMed PMID: 29750242; PubMed Central PMCID: PMCPMC6137996.

51. Lim CS, Sozzi V, Littlejohn M, Yuen LKW, Warner N, Betz-Stablein B, et al. Quantitative analysis of the splice variants expressed by the major hepatitis B virus genotypes. Microb Genom. 2021. Epub 2021/01/14. doi: 10.1099/mgen.0.000492. PubMed PMID: 33439114.

52. Belloni L, Pollicino T, De Nicola F, Guerrieri F, Raffa G, Fanciulli M, et al. Nuclear HBx binds the HBV minichromosome and modifies the epigenetic regulation of cccDNA function. Proc Natl Acad Sci U S A. 2009;106(47):19975-9. Epub 20091111. doi: 10.1073/pnas.0908365106. PubMed PMID: 19906987; PubMed Central PMCID: PMCPMC2775998.

53. Wing PA, Davenne T, Wettengel J, Lai AG, Zhuang X, Chakraborty A, et al. A dual role for SAMHD1 in regulating HBV cccDNA and RT-dependent particle genesis. Life Sci Alliance. 2019;2(2). Epub 20190327. doi: 10.26508/lsa.201900355. PubMed PMID: 30918010; PubMed Central PMCID: PMCPMC6438393.

Supporting information

Supplementary Figure 1. qPCR measurement of intracellular HBV DNA and pgRNA in transfected cells. HepG2-NTCP cells were transfected with HBV plasmids (4h) and cultured at 18% or 1% O_2 for 72h. (**A**) Total cellular DNA was extracted at 4h post-transfection and HBV DNA measured, normalized to *PrP* housekeeping gene and expressed relative to HBV WT. Data are presented as mean ± S.D. of n=3 from one of independent 3 experiments. (**B**) HBV pgRNA and *CA9* mRNAs were quantified by qPCR, expressed relative to *B2M* housekeeping gene with the data presented as mean ± S.D. of n=9 samples from 3 independent experiments, with statistical significance assessed using a non-parametric (Kruskall-Wallis) ANOVA, * $p < 0.05$, ** $p < 0.01$ *** $p < 0.001$, **** $p < 0.0001$.

Supplementary Figure 2. Liver zonation profile of a HIF pathway gene. Liver zonation profile of a HIF pathway gene, *Ndrg1*, based on scRNA-seq data of mouse liver [33].

Supplementary Figure 3. Efficiency of ALKBH5 siRNAs. Efficiency of siRNA #1 and #2 targeting ALKBH5. HepG2-NTCP cells transfected with siRNA (NC; Non-targeting, ALK; ALKBH5) for 6h and cultured at 18% or 1% O_2 for 72h and RNA extracted. *ALKBH5* RNA and protein levels were detected by qPCR and

bioRxiv preprint doi: https://doi.org/10.1101/2023.10.31.564956; this version posted November 1, 2023. The copyright holder for this preprint (which was not certified by peer review) is the author/funder, who has granted bioRxiv a license to display the preprint in perpetuity. It is made available under aCC-BY-NC-ND 4.0 International license.

western blotting, respectively. Statistical significance was assessed using Mann-Whitney tests, with Bonferroni correction for multiple comparisons, *** $p < 0.001$.

Supplementary Figure 4. *HIF-1α* mRNA methylation.

Methylated RNA immunoprecipitation (MeRIP) assay. HepG2-NTCP cells were incubated at 18% or 1% oxygen for 72h. RNA was extracted, treated with TURBO DNase and incubated overnight at 4℃ with protein A agarose beads with IgG or m^6A antibody. The beads were washed 5 times, and bound RNA eluted in 6.7 mM m^6A sodium salt, purified using a Qiagen RNA extract kit and *HIF-1α* transcripts measured by qPCR. Data are expressed relative to input total RNA and represent the mean ± S.D. of n=4 samples from 2 independent experiments.

Supplementary Figure 5. Hydroxylated HIF-1α protein expression in ALKBH5 silenced cells.

HepG2-NTCP cells were cultured at 1% oxygen for 24h and treated with MG132 (20 μM) for 4h. Samples were collected and probed for HIF-1α, ALKBH5 and β-Actin by western blotting.

Supplementary Table 1. HBV transcriptome analysis by long-read sequencing.

(A) HBV reads between samples. (B) HBV transcript frequencies.

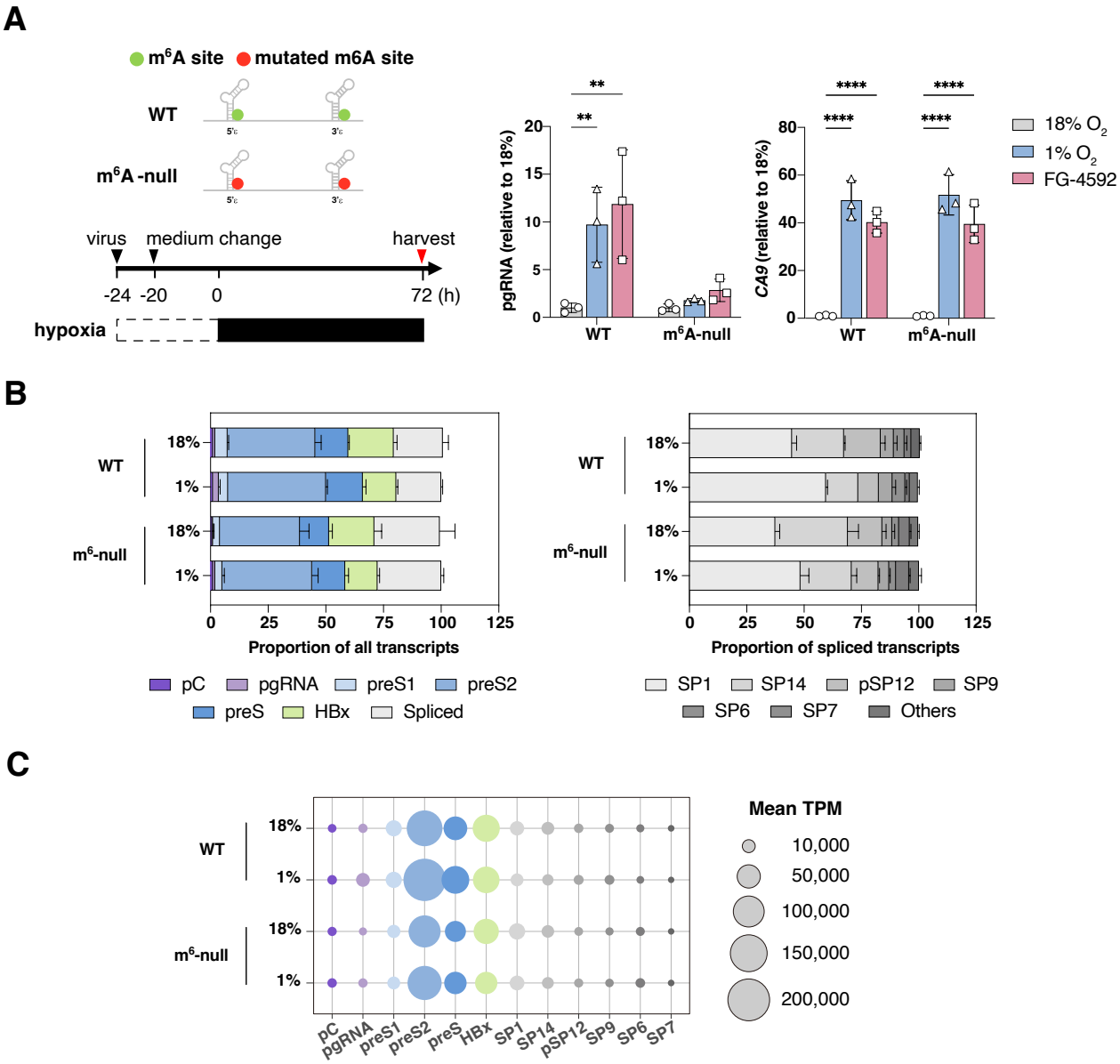

	pgRNA half life (h)		
	18% O_2	1% O_2	
WT	13.9 ± 2.18	12.2 ± 1.20	n.s.
m^{6}A-null	8.33 ± 2.18	6.93 ± 0.64	*

Figure.1

A

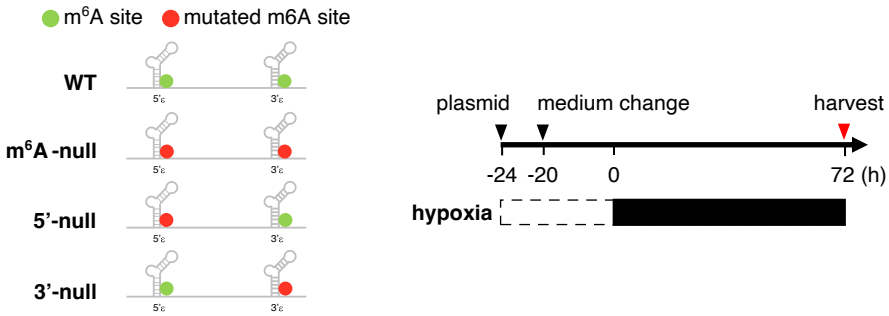

B

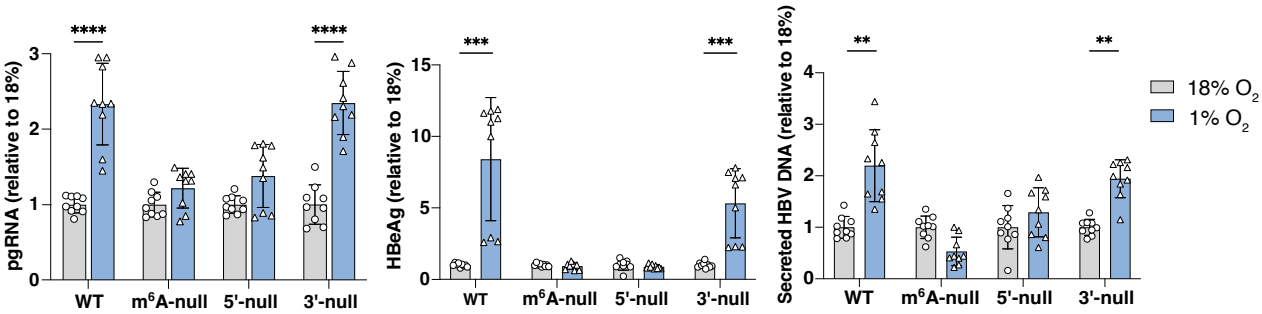

C

	pgRNA localization		
	Nucleus (%)	Capsid (%)	Cytosol (%)
18% O_2	4.69 ± 1.94	4.86 ± 1.65	90.4 ± 3.14
1% O_2	3.05 ± 1.26	4.76 ± 2.84	92.2 ± 2.34

Figure. 2

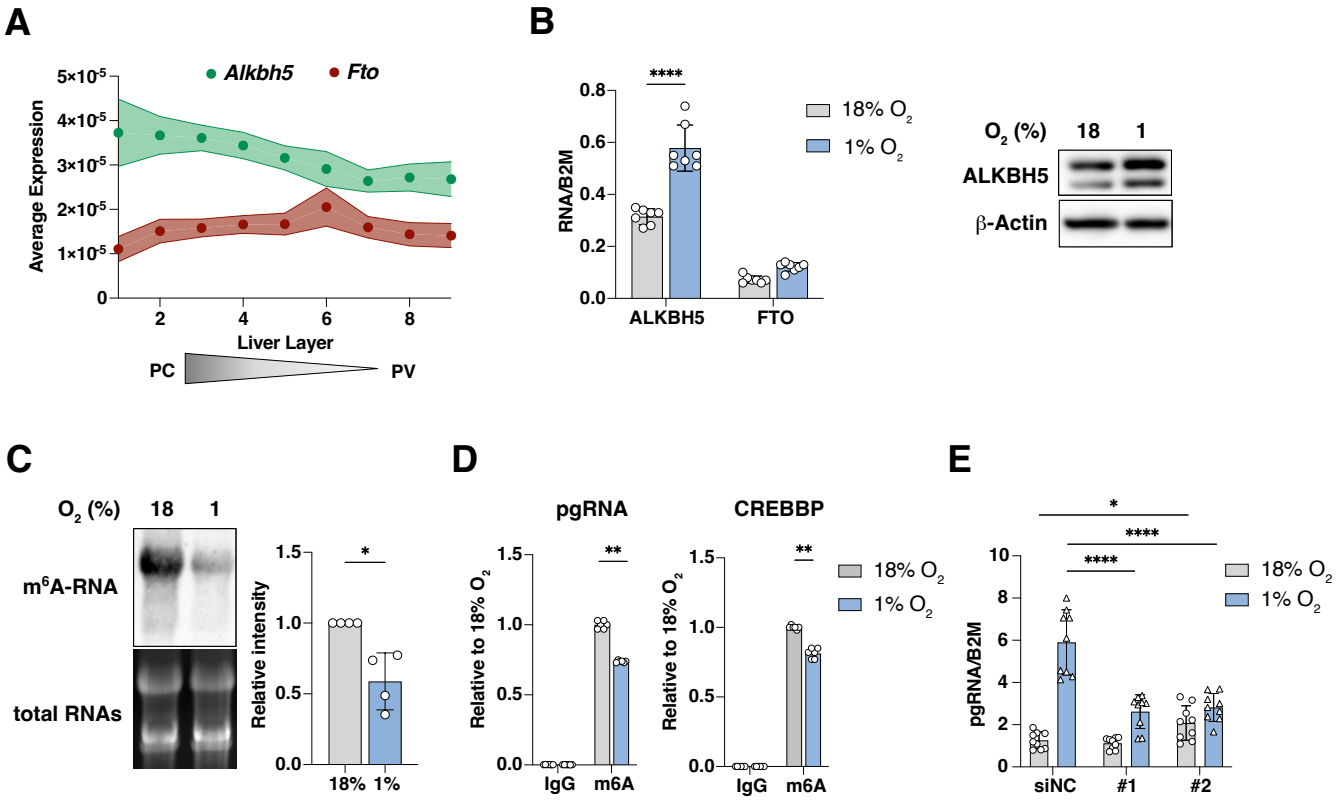
A
Alkbh5
Fto
Average Expression
5×10-5
4×10-5
3×10-5
2×10-5
1×10-5
0
2
4
6
8
Liver Layer
PC
PV
B
****
RNA/B2M
0.8
0.6
0.4
0.2
0.0
18% O2
1% O2
ALKBH5
FTO
O2 (%) 18 1
ALKBH5
β-Actin
C
O2 (%) 18 1
m6A-RNA
total RNAs
Relative intensity
1.5
1.0
0.5
0.0
*
18% 1%
D
pgRNA
CREBBP
Relative to 18% O2
**
IgG
m6A
18% O2
1% O2
E
*
****
****
pgRNA/B2M
10
8
6
4
2
0
siNC
#1
#2
18% O2
1% O2

Figure. 3

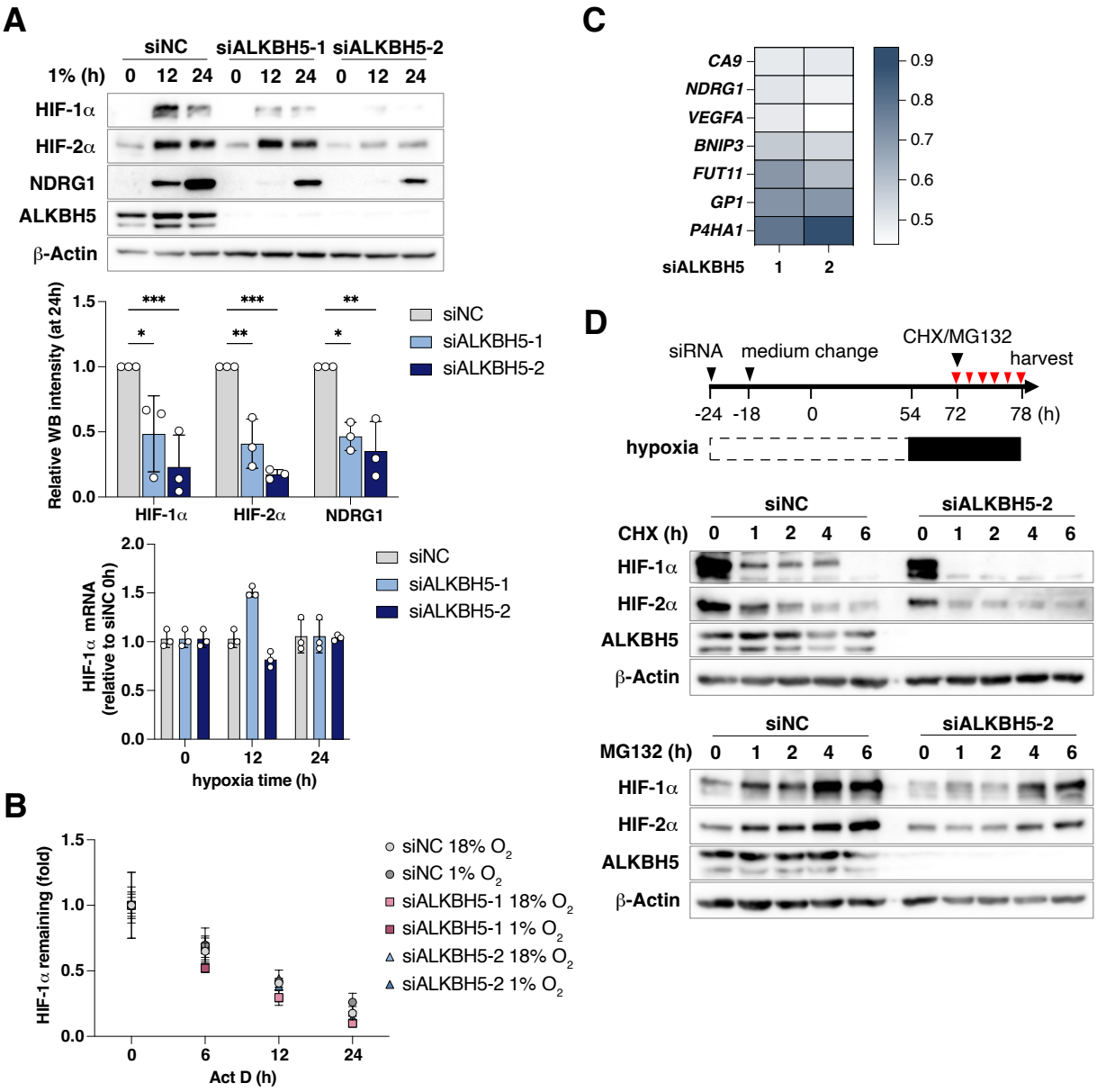
A
siNC
siALKBH5-1
siALKBH5-2
1% (h) 0 12 24 0 12 24 0 12 24
HIF-1α
HIF-2α
NDRG1
ALKBH5
β-Actin
Relative WB intensity (at 24h)
HIF-1α
HIF-2α
NDRG1
HIF-1α mRNA (relative to siNC 0h)
hypoxia time (h)
B
HIF-1α remaining (fold)
Act D (h)
siNC 18% O2
siNC 1% O2
siALKBH5-1 18% O2
siALKBH5-1 1% O2
siALKBH5-2 18% O2
siALKBH5-2 1% O2
C
CA9
NDRG1
VEGFA
BNIP3
FUT11
GP1
P4HA1
siALKBH5 1 2
D
siRNA
medium change
CHX/MG132
harvest
-24 -18 0 54 72 78 (h)
hypoxia
CHX (h) 0 1 2 4 6 0 1 2 4 6
MG132 (h) 0 1 2 4 6 0 1 2 4 6

Figure. 4

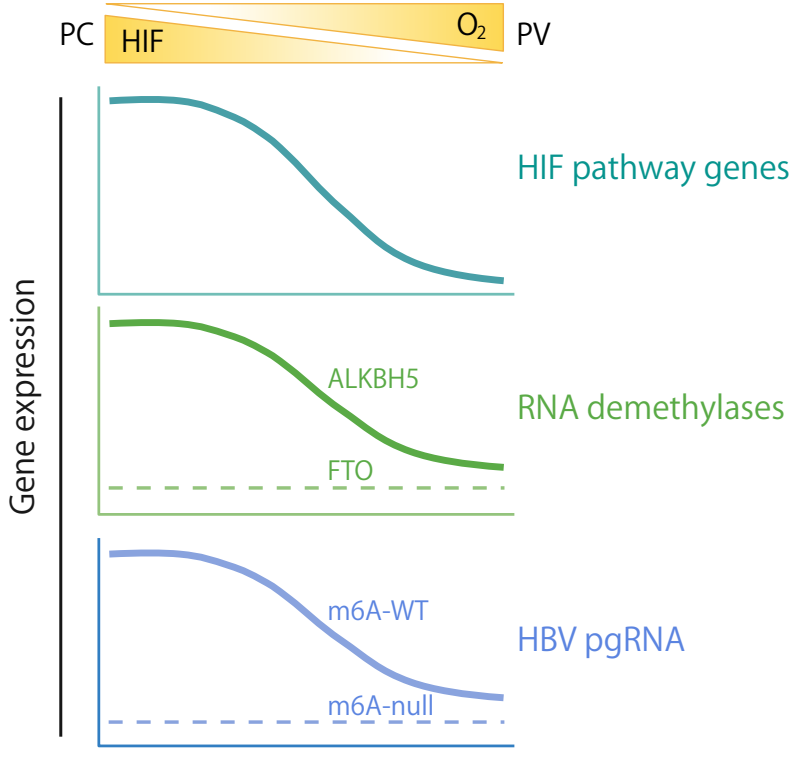
PC
HIF
O_2
PV
Gene expression
HIF pathway genes
ALKBH5
RNA demethylases
FTO
m6A-WT
HBV pgRNA
m6A-null

Figure. 5